

1. NEOGENE CALCAREOUS NANNOFOSSIL BIOSTRATIGRAPHY OF SITES 998, 999, AND 1000, CARIBBEAN SEA¹

Koji Kameo² and Timothy J. Bralower³

ABSTRACT

A total of 53 calcareous nannofossil datums were detected in Quaternary and Neogene sections recovered during Ocean Drilling Program Leg 165 in the Caribbean Sea. Most of the low-latitude nannofossil zonal markers of Okada and Bukry could be determined at all of the sites.

Additionally, size distribution patterns of specimens of *Reticulofenestra*, a common genus in Neogene and Quaternary sediments, were examined to interpret the biostratigraphic utility of changes in size.

INTRODUCTION

This paper documents the results of detailed calcareous nannofossil biostratigraphy of Neogene and Quaternary sediments recovered at three sites (Sites 998, 999, and 1000; Fig. 1 and Table 1) during Ocean Drilling Program (ODP) Leg 165 in the Caribbean Sea (Sigurdsson et al., 1997). The objectives of this study are (1) to describe the occurrence of stratigraphically important species, (2) to determine the boundaries of nannofossil zones, and (3) to provide an age model for the sections using standard biochronologies. In addition, detailed measurements of the size of specimens of *Reticulofenestra* were made to clarify stratigraphic changes and interpret their biostratigraphic utility.

METHODS

A total of 1826 samples were taken from Cores 165-998A-1H through 36X (339.4 meters below seafloor [mbsf]), 165-999A-1H through 61X (566.1 mbsf), and 165-1000A-1H through 59X (553.2 mbsf). Smear slides were prepared using standard techniques. Nannofossils were observed in a transmitted light microscope under cross-polarized light at a magnification of 1500 x. These observations were used to determine Neogene and Quaternary datums in three holes (Figs. 2, 3, 4).

The relative abundance of nannofossil species in the Neogene sections of Holes 998A and 999A was obtained based on detailed assemblage counts. Three hundred specimens were counted in most of the samples; in few samples with sparse nannofossils, 100–200 specimens were counted. Only quantitative assemblage data from Hole 998A are listed in Appendix B (back pocket). The overall preservation of nannofossils was described by using one of the following three designations: G = good preservation (fossils lack evidence of dissolution or overgrowth); M = moderately good preservation (fossils slightly etched are often observed); and P = poor preservation (most fossils are deeply etched or dissolved).

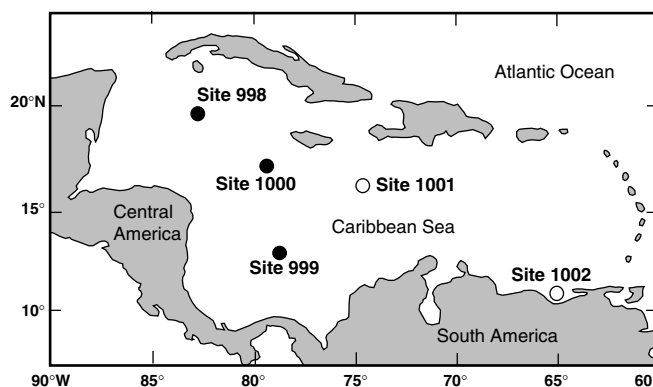


Figure 1. Location of the sites investigated. Solid circles = this study; open circles = other Leg 165 sites.

Table 1. Location and water depth of the sites studied.

Hole	Latitude	Longitude	Water depth (m)
998A	19°29.377'N	82°56.166'W	3179.9
999A	12°44.639'N	78°44.360'W	2827.9
1000A	16°33.223'N	79°52.044'W	915.9

Florisphaera profunda, a small nannofossil species present throughout the late Neogene and Quaternary, was not counted because this species is extremely abundant. The length of specimens of *Reticulofenestra* was measured using an eyepiece micrometer. The size distribution patterns of *Reticulofenestra* specimens are summarized in Figures 5 and 6.

ZONES AND DATUMS

Several calcareous nannofossil zonal schemes have been proposed for the subdivision of Cenozoic strata (e.g., Martini, 1971; Okada and Bukry, 1980). We chose the calcareous nannofossil zonal scheme of Bukry (1973, 1975) and Okada and Bukry (1980) to subdivide the Neogene and Quaternary sections of Holes 998A, 999A, and 1000A because this zonation was established largely on the basis of Carib-

¹Leckie, R.M., Sigurdsson, H., Acton, G.D., and Draper, G. (Eds.), 2000. *Proc. ODP, Sci. Results*, 165: College Station, TX (Ocean Drilling Program).

²Exploration Department, Teikoku Oil Co., Ltd., 1-31-10, Hatagaya, Shibuya, Tokyo, 151-8565 Japan. (Present address: Marine Biosystems Research Center, Chiba University, Uchiura 1, Amatsu-Kominato, Awa, Chiba, 299-5502 Japan. VYQ01434@nifty.ne.jp)

³Geology Department, University of North Carolina, Chapel Hill, NC 27599-3315, U.S.A.

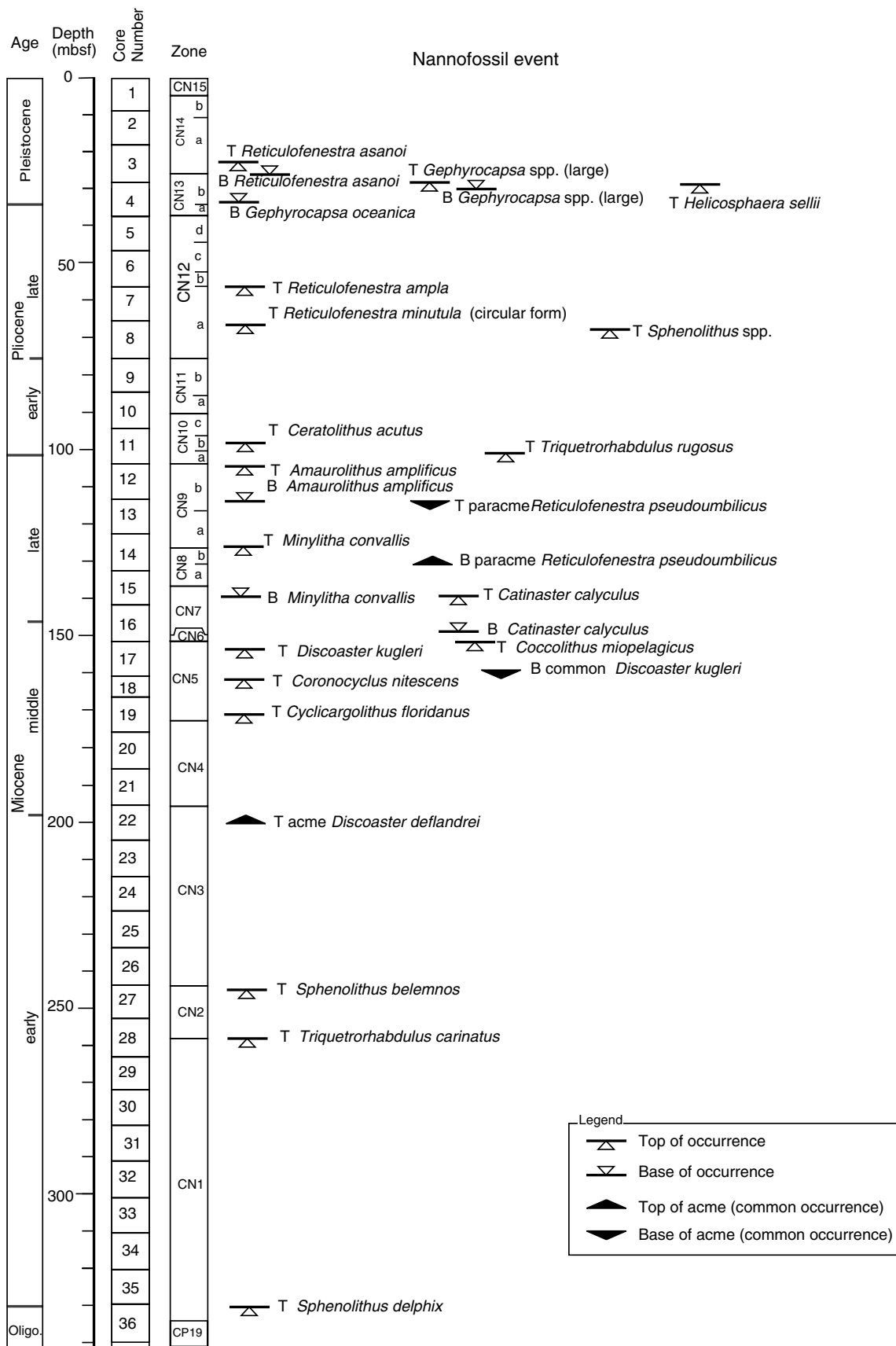


Figure 2. Stratigraphic positions of additional nannofossil datums in Hole 998A. Zonal markers are not shown in this figure.

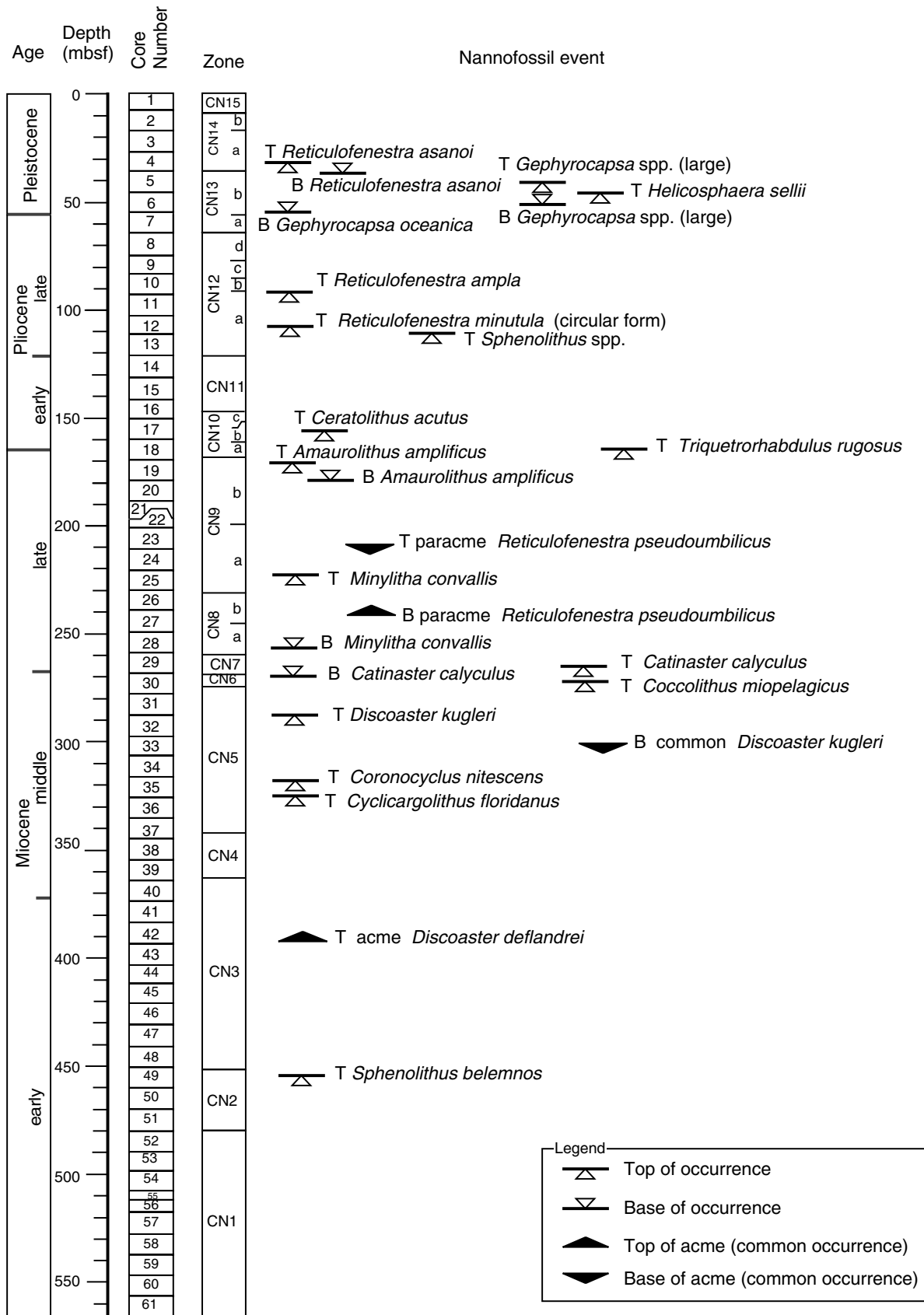


Figure 3. Stratigraphic positions of additional nannofossil datums in Hole 999A. Zonal markers are not shown in this figure.

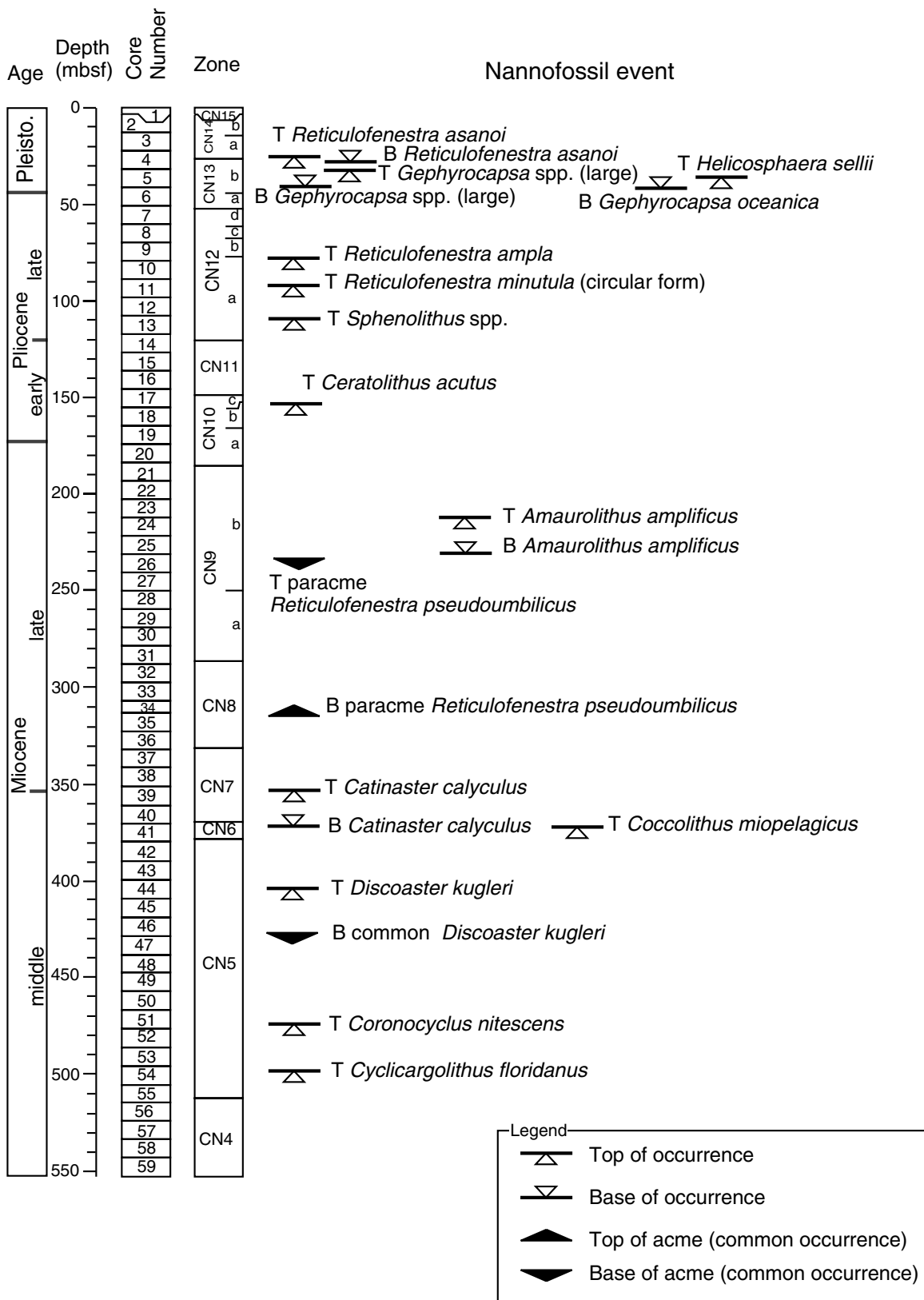


Figure 4. Stratigraphic positions of additional nannofossil datums in Hole 1000A. Zonal markers are not shown in this figure.

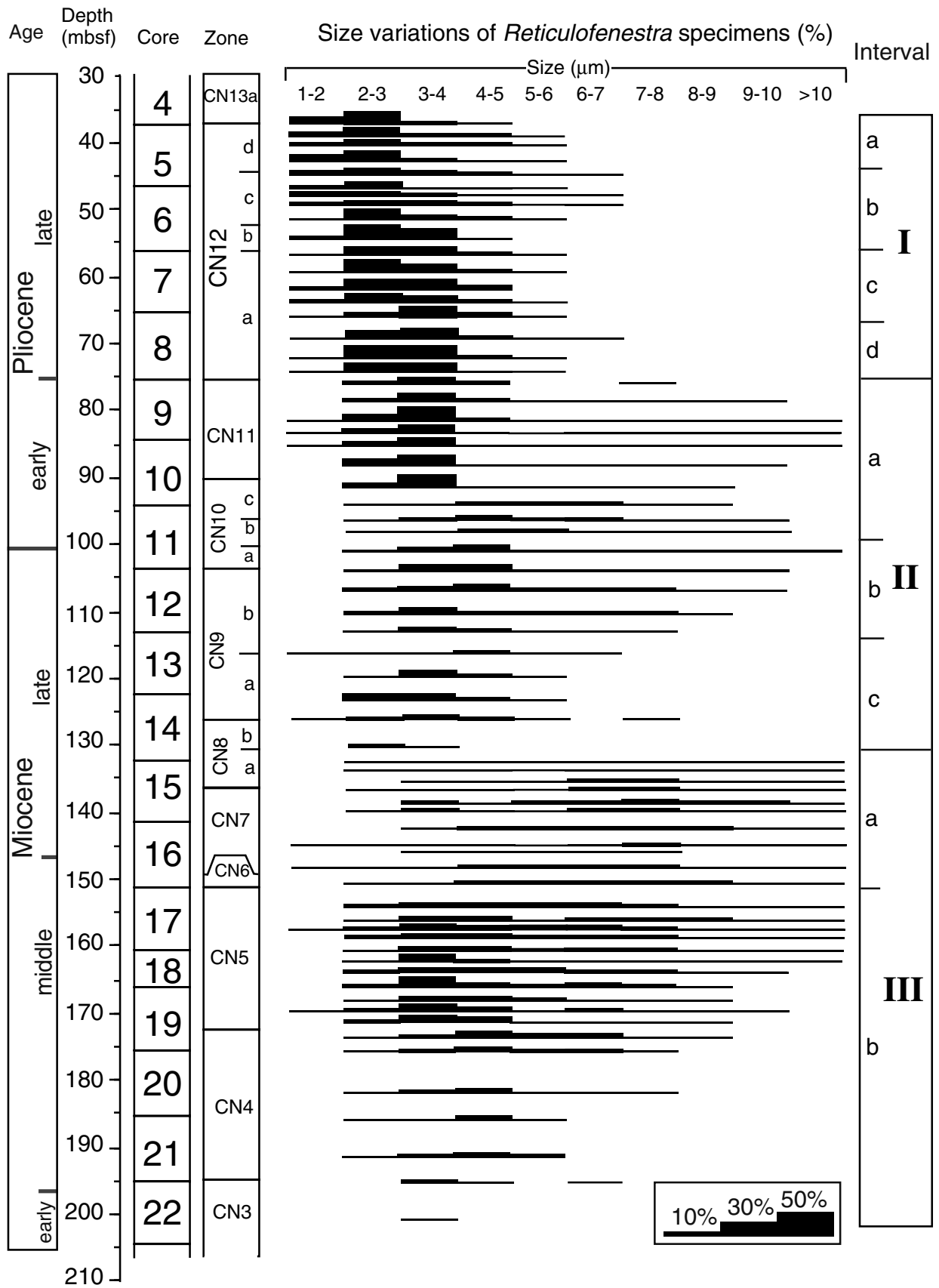


Figure 5. Size distributions of *Reticulofenestra* specimens at Site 998. Abundance of individual specimens shown in percent relative to total number of coccoliths.

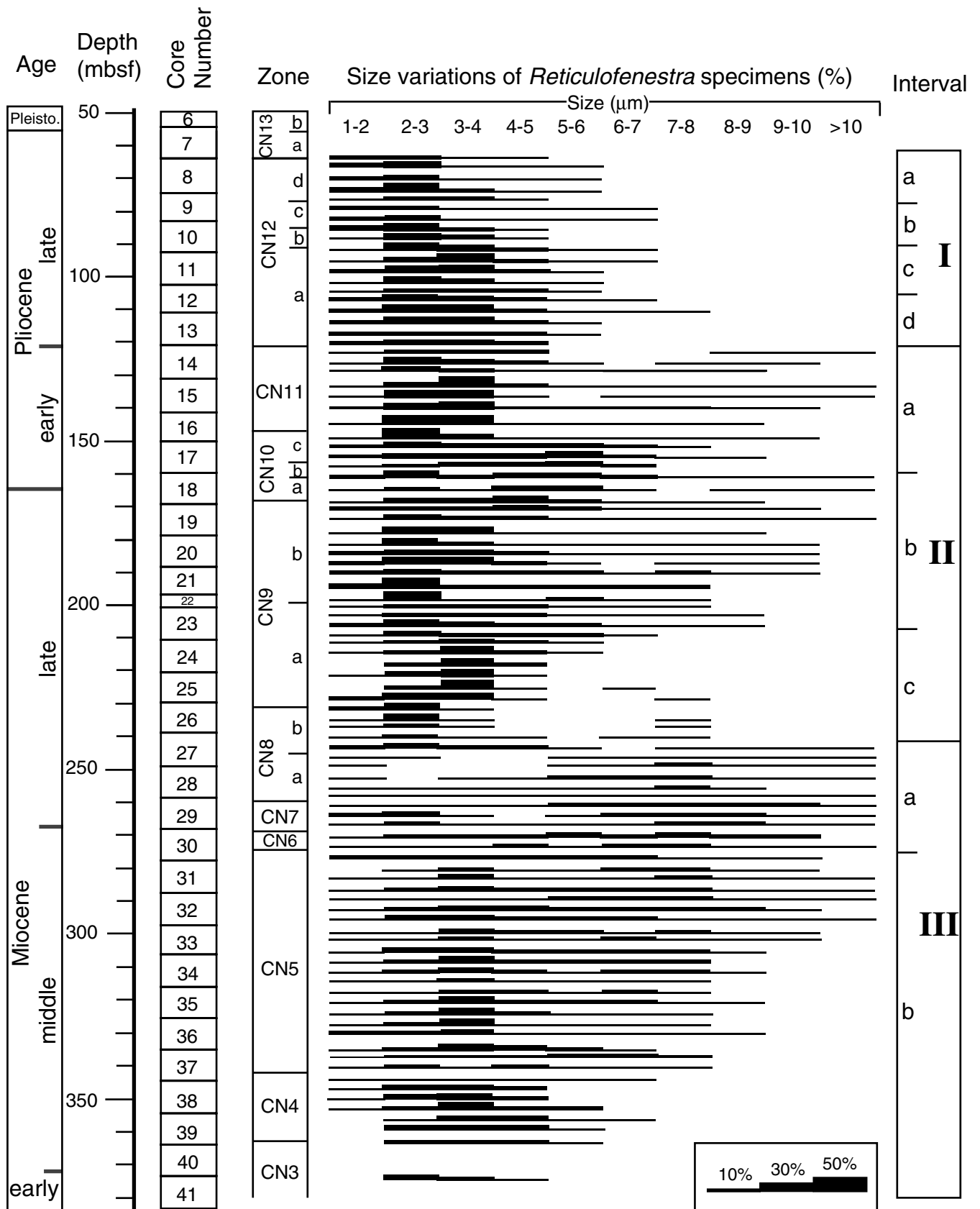


Figure 6. Size distributions of *Reticulofenestra* specimens at Site 999. Abundance of individual specimens shown in percent relative to total number of coccoliths.

bean sequences. Studies by Raffi and Flores (1995), Takayama et al. (1995), and Backman and Raffi (1997) of continuous sections in the eastern equatorial Pacific (ODP Leg 138), the Ontong Java Plateau (ODP Leg 130), and the Ceara Rise in the equatorial Atlantic (ODP Leg 154), respectively, have provided additional datums. The ages of most datums of Bukry (1973, 1975) and Okada and Bukry (1980) and other useful biohorizons were estimated using an orbitally tuned time scale (Backman and Raffi, 1997).

In this study, the ages of nannofossil datums and bioevents were taken from Raffi and Flores (1995) for the Miocene to lower Pliocene

and Takayama et al. (1995) for the upper Pliocene and Pleistocene (Table 2).

BIOSTRATIGRAPHIC SUMMARY

We observed well-preserved nannofossils throughout the cores (Appendix B, back pocket) except in the middle Miocene intervals where some samples contain poorly preserved nannofossils or are barren. This interval is characterized by dissolved assemblages and

Table 2. Ages of calcareous nannofossil events.

Datum and event	Zones (base)	Age (Ma)	Reference
B acme <i>Emiliana huxleyi</i>		0.085	1
T <i>Helicosphaera inversa</i>		0.16	2
B <i>Emiliana huxleyi</i>	CN15 NN21	0.25	2
T <i>Pseudoemiliana lacunosa</i>	CN14b NN20	0.41	2
B <i>Helicosphaera inversa</i>		0.51	2
T <i>Reticulofenestra asanoi</i>		0.85	2
B <i>Gephyrocapsa parallela</i>	CN14a	0.95	2
B <i>Reticulofenestra asanoi</i>		1.16	2
T <i>Gephyrocapsa</i> spp. (large)		1.21	2
T <i>Helicosphaera sellii</i>		1.27	2
B <i>Gephyrocapsa</i> spp. (large)		1.45	2
T <i>Calcidiscus macintyreii</i>		1.65	2
B <i>Gephyrocapsa oceanica</i>		1.65	2
B <i>Gephyrocapsa caribbeanica</i>	CN13b	1.73	2
T <i>Discoaster brouweri</i>	CN13a NN19	1.97	2
T <i>Discoaster pentaradiatus</i>	CN12d NN18	2.38	2
T <i>Discoaster surculus</i>	CN12c NN17	2.54	2
T <i>Discoaster tamalis</i>	CN12b	2.74	2
T <i>Reticulofenestra ampla</i>		2.78	2
T <i>Reticulofenestra minutula</i> (circ. form)		3.36	2
T <i>Sphenolithus</i> spp.		3.65	3
T <i>Reticulofenestra pseudoubilicus</i>	CN12a NN16	3.80	3
B acme <i>Discoaster asymmetricus</i>	CN11b	ND	
T <i>Amaurolithus primus</i>	CN11a NN15	4.37	4
B <i>Discoaster asymmetricus</i>		ND	
T <i>Ceratolithus acutus</i>	CN10c	5.04	5
B <i>Ceratolithus rugosus</i>	CN10c NN13	5.04	6
B <i>Ceratolithus acutus</i>	CN10b	5.34	3
T <i>Triquetrorhabdulus rugosus</i>	CN10b	5.34	3
T <i>Discoaster quinqueramus</i>	CN10a NN12	5.56	3
T <i>Amaurolithus amplifiscus</i>		5.88	3
B <i>Amaurolithus amplifiscus</i>		6.50	3
T paracme <i>Reticulofenestra pseudoubilicus</i>		6.80	3
B <i>Amaurolithus primus</i>	CN9b	7.24	3
T <i>Minylitha convallis</i>		7.80	7
B <i>Discoaster berggrenii</i>	CN9a NN11	8.35	3
B <i>Discoaster loeblichii</i>	CN8b	8.43	3
B paracme <i>Reticulofenestra pseudoubilicus</i>		8.85	3
T <i>Discoaster hamatus</i>	CN8a NN10	9.36	3
T <i>Catinaster calyculus</i>		9.36	5
B <i>Minylitha convallis</i>		9.43	3
B <i>Catinaster calyculus</i>	CN7b	10.70	7
B <i>Discoaster hamatus</i>	CN7a NN9	10.39	3
T <i>Coccolithus miopelagicus</i>		10.39	3
B <i>Catinaster coalitus</i>	CN6 NN8	10.71	3
T <i>Discoaster kugleri</i>		11.50	7
B common <i>Discoaster kugleri</i>		11.74	3
T <i>Coronocyclus nitescens</i>		12.12	3
B <i>Discoaster kugleri</i>	CN5b NN7	12.20	3
T <i>Cyclicargolithus floridanus</i>		13.19	3
T <i>Sphenolithus heteromorphus</i>	CN5a NN6	13.57	3
T <i>Helicosphaera ampliaptera</i>	CN4 NN5	15.83	8
T acme <i>Discoaster deflandrei</i>		16.21	3
B <i>Sphenolithus heteromorphus</i>	CN3	18.10	9
T <i>Sphenolithus belemnus</i>		18.40	9
B <i>Sphenolithus belemnus</i>	CN2	19.70	9
T <i>Triquetrorhabdulus carinatus</i>		23.10	9
B <i>Discoaster drugii</i>	CN1c NN2	23.20	7
T <i>Sphenolithus delphix</i>		23.80	7
T <i>Reticulofenestra bisecta</i>	CN1a	23.90	7

Notes: B acme = base of acme interval; T acme = top of acme interval; B paracme = base of paracme interval; T paracme = top of paracme interval; B = first occurrence; T = last occurrence; ND = no reliable data. References: 1 = Thierstein et al. (1977); 2 = modified from Takayama and Sato (1987), Sato et al. (1991), Takayama (1993), and Kameo et al. (1955) by using timescale of Cande and Kent (1995); 3 = Raffi and Flores (1995); 4 = Rio et al. (1990); 5 = Curry, Shackleton, Richter, et al. (1955); 6 = Backman and Shackleton (1983); 7 = Berggren et al. (1995); 8 = Backman et al. (1990); 9 = Olafsson (1991).

Table 3. Stratigraphic position of datums in Hole 998A.

Datum and bioevent	Zone (base)	Age (Ma)	Core, section, interval (cm)		Depth (mbsf)
			Upper	Lower	
B <i>Emiliana huxleyi</i>	CN15	0.25	165-998A-1H-4, 20	165-998A-1H-4, 70	4.95
T <i>Pseudoemiliana lacunosa</i>	CN14b	0.41	2H-1, 100	2H-2, 20	10.15
T <i>Reticulofenestra asanoi</i>		0.85	3H-3, 121	3H-4, 18	22.75
B <i>Gephyrocapsa parallela</i>	CN14a	0.95	3H-5, 120	3H-6, 20	25.75
B <i>Reticulofenestra asanoi</i>		1.16	3H-6, 20	3H-6, 70	26.25
T <i>Gephyrocapsa</i> spp. (large)		1.21	3H-CC	4H-1, 83	28.22
T <i>Helicosphaera sellii</i>		1.27	4H-1, 70	4H-1, 100	28.65
B <i>Gephyrocapsa</i> spp. (large)		1.45	4H-2, 20	4H-2, 70	29.75
B <i>Gephyrocapsa oceanica</i>		1.65	4H-4, 120	4H-5, 20	33.75
T <i>Calcidiscus macintyreii</i>		1.65	4H-4, 120	4H-5, 20	33.75
B <i>Gephyrocapsa caribbeanica</i>	CN13b	1.73	4H-5, 70	4H-6, 100	35.40
T <i>Discoaster browneri</i>	CN13a	1.97	4H-CC	5H-1, 20	37.40
T <i>Discoaster pentaradiatus</i>	CN12d	2.38	5H-5, 100	5H-6, 20	44.65
T <i>Discoaster surculus</i>	CN12c	2.54	6H-4, 100	6H-5, 20	52.65
T <i>Discoaster tamalis</i>	CN12b	2.74	6H-CC	7H-1, 20	56.40
T <i>Reticulofenestra ampla</i>		2.78	6H-CC	7H-1, 20	56.40
T <i>Reticulofenestra minutula</i> (circ. form)		3.36	8H-1, 20	8H-1, 100	66.40
T <i>Sphenolithus</i> spp.		3.65	8H-1, 100	8H-2, 20	67.15
T <i>Reticulofenestra pseudoubilicus</i>	CN12a	3.80	8H-7, 60	8H-CC	75.30
B acme <i>Discoaster asymmetricus</i>	CN11b		10H-1, 20	10H-2, 19	85.75
T <i>Amaurolithus tricorniculatus</i>	CN11a	4.37	10H-4, 100	10H-5, 20	90.65
B <i>Ceratolithus rugosus</i>	CN10c	5.04	11H-2, 20	11H-2, 100	96.40
T <i>Ceratolithus acutus</i>	CN10e	5.04	11H-3, 20	11H-4, 20	98.25
B <i>Ceratolithus acutus</i>	CN10b	5.34	11H-4, 100	11H-5, 20	100.15
T <i>Triquetrorhabdulus rugosus</i>	CN10b	5.34	11H-5, 20	11H-6, 20	101.25
T <i>Discoaster quinquerramus</i>	CN10a	5.56	11H-CC	12H-1, 19	103.90
T <i>Amaurolithus amplifolius</i>		5.88	12H-1, 100	12H-2, 20	105.15
T paracme <i>Reticulofenestra pseudoubilicus</i>		6.80	12H-CC	13H-1, 20	113.40
B <i>Amaurolithus amplifolius</i>		6.50	13H-1, 20	13H-1, 100	113.90
B <i>Amaurolithus</i> spp.	CN9b	7.24	13H-3, 10	13H-3, 100	116.85
T <i>Minylitha convallis</i>		7.80	14H-3, 20	14H-3, 100	126.40
B <i>Discoaster berggrenii</i>	CN9a	8.35	14H-3, 20	14H-3, 100	126.40
B paracme <i>Reticulofenestra pseudoubilicus</i>		8.85	14H-6, 23	14H-6, 100	130.92
B <i>Discoaster loeblichii</i>	CN8b	8.43	14H-6, 23	14H-6, 100	130.92
T <i>Discoaster hamatus</i>	CN8a	9.36	15H-3, 100	15H-4, 20	136.65
B <i>Minylitha convallis</i>		9.43	15H-5, 20	15H-6, 20	139.25
T <i>Catinaster calyculus</i>		9.36	15H-5, 20	15H-6, 20	139.25
B <i>Catinaster calyculus</i>	CN7b	10.70	16H-5, 20	16H-5, 100	148.40
B <i>Discoaster hamatus</i>	CN7a	10.39	16H-5, 100	16H-6, 20	149.15
T <i>Coccolithus miopelagicus</i>		10.39	16H-CC	17H-1, 20	151.40
B <i>Catinaster coalitus</i>	CN6	10.71	16H-CC	17H-1, 20	151.40
T <i>Discoaster kugleri</i>		11.50	17H-2, 20	17H-2, 100	153.40
B common <i>Discoaster kugleri</i>		11.74	17H-5, 20	17H-5, 100	157.90
T <i>Coronocyclus ntescens</i>		12.12	18H-1, 20	18H-2, 20	161.75
T <i>Cycliargolithus floridanus</i>		13.19	19X-4, 20	19X-4, 100	171.30
T <i>Sphenolithus heteromorphus</i>	CN5a	13.57	19X-5, 20	19X-5, 80	172.70
T <i>Helicosphaera ampliapertura</i>	CN4	15.83	21X-CC	22X-1, 67	195.44
T acme <i>Discoaster deflandrei</i>		16.21	22X-4, 20	22X-5, 20	200.55
B <i>Sphenolithus heteromorphus</i>	CN3	18.10	26X-CC	27X-1, 100	242.56
T <i>Sphenolithus belemnus</i>		18.40	27X-1, 100	27X-2, 100	244.95
B <i>Sphenolithus belemnus</i>	CN2	19.70	28X-3, 100	28X-4, 100	257.65
T <i>Triquetrorhabdulus carinatus</i>		18.95	28X-3, 100	28X-4, 100	257.65
T <i>Sphenolithus delphix</i>		23.80	35X-CC	36X-1, 100	330.01
T <i>Reticulofenestra bisecta</i>	CN1a	23.90	36X-2, 100	36X-3, 100	333.05

Note: See Table 2 for definitions and reference descriptions.

corresponds to the “middle Miocene Carbonate Crash” interval, which was also observed in the eastern equatorial Pacific cores (Lyle et al., 1995). Stratigraphic positions of datums recognized in the three holes are shown in Tables 3–5.

Quaternary

Zone CN15 (*Emiliana huxleyi* Zone)

Hole 998A: above Sample 165-998A-1H-4, 20 cm
 Hole 999A: above Sample 165-999A-2H-1, 100 cm
 Hole 1000A: above Sample 165-1000A-1H-CC

The base of this zone is defined by the first occurrence (FO) of *Emiliana huxleyi*. Two other datums, the base of the acme of *E. huxleyi* and the last occurrence (LO) of *Helicosphaera inversa*, have not been determined. The former event was difficult to identify because the abundance of *E. huxleyi* increased gradually; *Helicosphaera inversa* was rare and had a sporadic stratigraphic occurrence in the three holes.

Zone CN14 (*Gephyrocapsa oceanica* Zone)

Hole 998A: interval 165-998A-1H-4, 70 cm, to 3H-5, 120 cm
 Hole 999A: interval 165-999A-2H-1, 122 cm, to 4H-6, 100 cm
 Hole 1000A: interval 165-1000A-2H-1, 50 cm, to 4H-3, 50 cm

The top of this zone is defined by the FO of *E. huxleyi*, and the base is approximated using the FO of *Gephyrocapsa parallela*. Bukry (1973, 1975) defined the base of Zone CN14 by the FO of *Gephyrocapsa oceanica*, but the base of this zone might correspond to the FO of *G. parallela* (Takayama and Sato, 1987). The FO of *G. parallela* almost coincides with the re-entrance of medium-sized *Gephyrocapsa* (Raffi et al., 1993) and the FO of *Gephyrocapsa* sp. 3 (Rio, 1982); the latter taxon corresponds to “*G. omega* - *G. parallela* morphotypes” (Raffi et al., 1993). *G. oceanica*, used as the definition of the base of Zone CN14 by Bukry (1973, 1975), is considered to be *G. parallela* because Bukry (1973) reported only the presence of “*G. omega*” within the *Gephyrocapsa oceanica* Zone (CN14 by Okada and Bukry, 1980).

Table 4. Stratigraphic position of datums in Hole 999A.

Datum and bioevent	Zone (base)	Age (Ma)	Core, section, interval (cm)		Depth (mbsf)
			Upper	Lower	
			165-999A-	165-999A-	
B <i>Emiliana huxleyi</i>	CN15	0.25	2H-1, 100	2H-1, 122	8.71
T <i>Pseudoemiliana lacunosa</i>	CN14b	0.41	2H-7, 30	2H-CC	17.00
T <i>Reticulofenestra asanoi</i>		0.85	4H-4, 22	4H-4, 72	31.57
B <i>Gephyrocapsa parallela</i>	CN14a	0.95	4H-6, 100	4H-7, 30	35.50
B <i>Reticulofenestra asanoi</i>		1.16	5H-1, 72	5H-1, 100	36.96
T <i>Gephyrocapsa</i> spp. (large)		1.21	5H-4, 22	5H-4, 72	41.07
T <i>Helicosphaera sellii</i>		1.27	5H-7, 30	5H-CC	45.50
B <i>Gephyrocapsa</i> spp. (large)		1.45	6H-4, 100	6H-4, 122	51.21
B <i>Gephyrocapsa oceanica</i>		1.65	7H-1, 22	7H-1, 72	55.57
T <i>Calcidiscus macintyreii</i>		1.65	7H-1, 22	7H-1, 72	55.57
B <i>Gephyrocapsa caribbeanica</i>	CN13b	1.73	7H-1, 100	7H-1, 122	56.21
T <i>Discoaster brouweri</i>	CN13a	1.97	7H-CC	8H-1, 100	65.10
T <i>Discoaster pentaradiatus</i>	CN12d	2.38	9H-3, 72	9H-3, 122	78.07
T <i>Discoaster surculus</i>	CN12c	2.54	10H-1, 122	10H-2, 22	85.07
T <i>Discoaster tamalis</i>	CN12b	2.74	10H-5, 122	10H-6, 21	91.07
T <i>Reticulofenestra ampla</i>		2.78	10H-5, 122	10H-6, 21	91.07
T <i>Reticulofenestra minutula</i> (circ. form)		3.36	12H-4, 72	12H-5, 22	108.32
T <i>Sphenolithus</i> spp.		3.65	13H-1, 122	13H-2, 22	113.57
T <i>Reticulofenestra pseudoumbilicus</i>	CN12a	3.80	13H-6, 100	13H-7, 30	121.00
T <i>Amurolithus primus</i>	CN11a	4.37	16H-5, 100	16H-6, 22	147.96
B <i>Ceratolithus rugosus</i>	CN10c	5.04	16H-CC	17H-1, 100	150.60
T <i>Ceratolithus acutus</i>	CN10e	5.04	17H-5, 100	17H-6, 22	157.46
B <i>Ceratolithus acutus</i>	CN10b	5.34	18H-1, 100	18H-2, 22	160.96
T <i>Triquetrorhabdulus rugosus</i>		5.34	18H-2, 100	18H-3, 22	162.46
T <i>Discoaster quinqueramus</i>	CN10a	5.56	18H-6, 100	18H-7, 30	168.50
T <i>Amurolithus amplifiscus</i>		5.88	19H-1, 100	19H-2, 22	170.46
B <i>Amurolithus amplifiscus</i>		6.50	19H-7, 22	19H-CC	178.46
B <i>Amurolithus</i> spp.	CN9b	7.24	22X-2, 22	22X-2, 100	199.71
T paracme <i>Reticulofenestra pseudoumbilicus</i>		6.80	23X-6, 22	23X-7, 22	209.07
T <i>Minyolitha convallis</i>		6.70	25X-2, 23	25X-3, 21	223.90
B <i>Discoaster berggrenii</i>	CN9a	8.35	26X-2, 22	26X-2, 100	231.61
B paracme <i>Reticulofenestra pseudoumbilicus</i>		8.85	27X-2, 24	27X-3, 24	241.59
B <i>Discoaster loeblichii</i>	CN8b	8.43	27X-5, 22	27X-5, 100	245.71
B <i>Minyolitha convallis</i>		9.43	28X-6, 22	28X-7, 22	257.17
T <i>Discoaster hamatus</i>	CN8a	9.36	29X-1, 22	29X-1, 100	259.01
T <i>Catinaster calyculus</i>		9.36	29X-6, 22	29X-7, 22	266.87
B <i>Discoaster hamatus</i>	CN7a	10.39	29X-CC	30X-1, 22	268.11
B <i>Catinaster calyculus</i>	CN7b	10.70	30X-2, 21	30X-3, 21	270.46
T <i>Coccolithus miopelagicus</i>		10.39	30X-3, 100	30X-4, 21	272.36
B <i>Catinaster coalitus</i>	CN6	10.71	30X-5, 21	30X-5, 100	274.61
T <i>Discoaster kugleri</i>		11.50	31X-CC	32X-1, 22	287.31
B common <i>Discoaster kugleri</i>		11.74	33X-6, 100	33X-7, 30	305.60
T <i>Coronocyclus nitescens</i>		12.12	35X-2, 24	35X-3, 23	318.49
T <i>Cyclicargolithus floridanus</i>		13.19	35X-7, 20	35X-CC	325.40
T <i>Sphenolithus heteromorphus</i>	CN5a	13.57	37X-5, 100	37X-6, 22	342.56
T <i>Helicosphaera ampliapertura</i>	CN4	15.83	39X-7, 30	39X-CC	363.85
T acme <i>Discoaster deflandrei</i>		16.21	42X-5, 100	42X-CC	391.70
B <i>Sphenolithus heteromorphus</i>	CN3	18.10	48X-CC	49X-1, 100	451.30
T <i>Sphenolithus belemnus</i>		18.40	49X-3, 100	49X-4, 100	454.95
B <i>Sphenolithus belemnus</i>	CN2	19.70	51X-CC	52X-1, 100	480.10
T <i>Reticulofenestra bisecta</i>	CN1a	23.90	Below base of section		

Note: See Table 2 for definitions and reference descriptions.

Two other useful datums, the LOs of *Pseudoemiliana lacunosa* and *Reticulofenestra asanoi*, lie in Zone CN14. The LO of *P. lacunosa* defines the boundary between Subzones CN14b (*Ceratolithus cristatus* Subzone) and CN14a (*Emiliana ovata* Subzone).

Zone CN13 (*Crenolithus doronicoides* Zone)

Hole 998A: interval 165-998A-3H-6, 20 cm, to 4H-CC
 Hole 999A: interval 165-999A-4H-7, 30 cm, to 7H-CC
 Hole 1000A: interval 165-1000A-4H-4, 50 cm, to 7H-1, 50 cm

This interval lies between the LO of *Discoaster brouweri* and the FO of *G. parallela*. Some of the datums defined by Takayama and Sato (1987) can be used to subdivide this interval and to correlate between the three sites. For example, the FO of *Gephyrocapsa caribbeanica* (= FO of medium *Gephyrocapsa* spp. by Raffi et al. [1993]) defines the boundary between Subzones CN13b (*Gephyrocapsa caribbeanica* Subzone) and CN13a (*Emiliana annula* Subzone) and approximates the Pliocene/Pleistocene boundary. Thus, the Pliocene/Pleistocene boundary should be placed close to the intervals corre-

sponding to Samples 165-998A-4H-5, 70 cm; 165-999A-4H-7, 30 cm; and 165-1000A-4H-4, 50 cm.

Pliocene

Zone CN12 (*Discoaster brouweri* Zone)

Hole 998A: interval 165-998A-5H-1, 20 cm, to 8H-7, 60 cm
 Hole 999A: interval 165-999A-8H-1, 100 cm, to 13H-6, 100 cm
 Hole 1000A: interval 165-1000A-7H-2, 50 cm, to 14H-2, 50 cm

This zone lies between the LO of *Reticulofenestra pseudoumbilicus* and the LO of *Discoaster brouweri*. It is subdivided into four subzones by the subsequent LOs of *Discoaster pentaradiatus*, *D. surculus*, and *D. tamalis* (Bukry, 1973, 1975; Okada and Bukry, 1980). All of these datums have been determined in the Caribbean cores (see Tables 3–5). In addition, the FO of *Discoaster triradiatus*, a three-rayed discoaster, lies in the uppermost part of the Pliocene (Takayama, 1970). Similarly, Backman and Shackleton (1983) used the increase in abundance of *D. triradiatus* relative to *D. brouweri* as an event in the uppermost Pliocene. This species was observed in the

Table 5. Stratigraphic position of datums in Hole 1000A.

Datum and bioevent	Zone (base)	Age (Ma)	Core, section, interval (cm)		Depth (mbsf)
			Upper	Lower	
B <i>Emiliana huxleyi</i>	CN15	0.25	165-1000A-1H-CC	165-1000A-2H-1, 50	3.55
T <i>Pseudoemiliana lacunosa</i>	CN14b	0.41	3H-1, 50	3H-2, 50	14.05
T <i>Reticulofenestra asanoi</i>		0.85	4H-2, 50	4H-3, 50	25.05
B <i>Gephyrocapsa parallela</i>	CN14a	0.95	4H-3, 50	4H-4, 50	26.55
B <i>Reticulofenestra asanoi</i>		1.16	4H-4, 50	4H-5, 50	28.05
T <i>Gephyrocapsa</i> spp. (large)		1.21	4H-CC	5H-1, 50	32.05
T <i>Helicosphaera sellii</i>		1.27	5H-3, 50	5H-4, 50	36.05
B <i>Gephyrocapsa</i> spp. (large)		1.45	5H-6, 50	5H-6, 130	40.20
B <i>Gephyrocapsa oceanica</i>		1.65	5H-6, 130	5H-CC	40.95
T <i>Calcidiscus macintyreii</i>		1.65	5H-6, 130	5H-CC	40.95
B <i>Gephyrocapsa caribbeanica</i>	CN13b	1.73	6H-2, 50	6H-3, 50	44.05
T <i>Discoaster brouweri</i>	CN13a	1.97	7H-1, 50	7H-2, 50	52.05
T <i>Discoaster pentaradiatus</i>	CN12d	2.38	8H-1, 50	8H-2, 50	61.55
T <i>Discoaster surculus</i>	CN12c	2.54	8H-5, 50	8H-6, 50	67.55
T <i>Discoaster tamalis</i>	CN12b	2.74	9H-5, 50	9H-6, 50	77.05
T <i>Reticulofenestra ampla</i>		2.78	9H-6, 50	9H-7, 50	78.55
T <i>Reticulofenestra minutula</i> (circ. form)		3.36	11H-2, 50	11H-3, 50	91.55
T <i>Sphenolithus</i> spp.		3.65	13H-1, 60	13H-2, 60	109.15
T <i>Reticulofenestra pseudoubilicus</i>	CN12a	3.80	14H-2, 50	14H-3, 50	120.05
T <i>Amaurolithus primus</i>	CN11a	4.37	17H-2, 50	17H-3, 50	148.55
B <i>Ceratolithus rugosus</i>	CN10c	5.04	17H-4, 50	17H-5, 50	151.55
T <i>Ceratolithus acutus</i>	CN10c	5.04	17H-5, 50	17H-6, 50	153.05
B <i>Ceratolithus acutus</i>	CN10b	5.34	19H-1, 50	19H-2, 50	166.05
T <i>Discoaster quinqueramus</i>	CN10a	5.56	21H-1, 50	21H-2, 50	185.05
T <i>Amaurolithus amplificus</i>		5.88	23H-CC	24H-1, 50	212.55
B <i>Amaurolithus amplificus</i>		6.50	25H-7, 50	25X-CC	231.30
T paracme <i>Reticulofenestra pseudoubilicus</i>		6.80	26H-1, 50	26H-2, 50	232.55
B <i>Amaurolithus</i> spp.	CN9b	7.24	27H-CC	28H-1, 50	250.55
B <i>Discoaster berggrenii</i>	CN9a	8.35	31H-5, 50	31H-6, 50	286.05
B paracme <i>Reticulofenestra pseudoubilicus</i>		8.85	35X-1, 51	35X-2, 49	314.15
T <i>Discoaster hamatus</i>	CN8a	9.36	36X-6, 50	36X-CC	331.30
T <i>Catinaster calyculus</i>		9.36	39X-1, 50	39X-2, 50	352.55
B <i>Discoaster hamatus</i>	CN7a	10.39	40X-6, 50	40X-CC	369.70
B <i>Catinaster calyculus</i>	CN7b	10.70	40X-CC	41X-1, 50	370.75
T <i>Coccolithus miopelagicus</i>		10.39	41X-1, 50	41X-2, 50	371.75
B <i>Catinaster coalitus</i>	CN6	10.71	41X-5, 50	41X-6, 50	377.25
T <i>Discoaster kugleri</i>		11.50	44X-3, 50	44X-4, 50	403.65
B common <i>Discoaster kugleri</i>		11.74	46X-CC	47X-1, 50	428.55
T <i>Coronocyclus nitescens</i>		12.12	51X-5, 50	51X-6, 50	473.95
T <i>Cyclicargolithus floridanus</i>		13.19	54X-2, 50	54X-3, 50	498.35
T <i>Sphenolithus heteromorphus</i>	CN5a	13.57	55X-6, 50	55X-CC	514.00
T <i>Helicosphaera ampliaptera</i>	CN4	15.83	Below base of section		

Note: See Table 2 for definitions and reference descriptions.

uppermost part of Subzone CN12d (*Calcidiscus macintyreii* Subzone) in the Caribbean sites, but it is too rare to determine the abundance increase event defined by Backman and Shackleton (1983).

Two other events can be identified in this zone in the Caribbean sections: the LOs of *Reticulofenestra ampla* and a circular form of *Reticulofenestra minutula*. These events were described by Sato et al. (1991) in sections from the North Atlantic and the Indian Oceans. *R. ampla* is a small form of *Reticulofenestra pseudoubilicus* with a diameter >5 µm (Figs. 5, 6). This species is one of the "medium reticulofenestrids" defined by Flores et al. (1995) at Sites 849 and 852 in the eastern equatorial Pacific. The LO of *R. ampla* lies at about the same level as the LO of *Discoaster tamalis*, which defines the top of Subzone CN12a (*Discoaster tamalis* Subzone). The occurrence of the circular form of *R. minutula* is limited to the lower part of Subzone CN12a in the Caribbean. The size of the circular form of *R. minutula* is >5 µm in diameter.

The LO of *Sphenolithus* spp, including *Sphenolithus abies* and *Sphenolithus neoabies*, lies in the lower part of Subzone CN12a in all of the studied sections. This event, however, lies slightly above the LO of *Reticulofenestra pseudoubilicus*, which defines the base of Zone CN12. This event was used by Bukry (1991) for the further subdivision of Subzone CN12a in Subzones CN12aA and CN12aB.

Zone CN11 (*Reticulofenestra pseudoubilicus* Zone)

Hole 998A: interval 165-998A-8H-CC, to 10H-4, 100 cm
 Hole 999A: interval 165-999A-13H-7, 30 cm, to 16H-5, 100 cm
 Hole 1000A: interval 165-1000A-14H-3, 50 cm, to 17H-2, 50 cm

This zone lies between the LO of *Amaurolithus* spp. and the LO of *Reticulofenestra pseudoubilicus*. One of the most prominent datums in the Pliocene sequence at the Caribbean sites is the LO of *R. pseudoubilicus* (Tables 3–5). Many authors define this event as the LO of large (>7 µm in diameter) *Reticulofenestra* specimens (e.g., Raffi and Flores, 1995). *R. pseudoubilicus* and *Sphenolithus* spp. are both abundant in Zone CN11. Bukry (1973) described the beginning of abundant occurrence of *Discoaster asymmetricus* within Zone CN11 and used it for the subdivision of Zone CN11. We were able to recognize this datum only in Hole 998A.

Zone CN10 (*Amaurolithus tricorniculatus* Zone)

Hole 998A: interval 165-998A-10H-5, 20 cm, to 11H-CC
 Hole 999A: interval 165-999A-16H-6, 22 cm, to 18H-6, 100 cm
 Hole 1000A: interval 165-1000A-17H-3, 50 cm, to 21H-1, 50 cm

This zone lies between the LO of *Discoaster quinqueramus* and the LO of *Amaurolithus* spp. Originally, Bukry (1973) used the LOs of *Amaurolithus tricorniculatus* and *Amaurolithus primus* as the boundary definition for the top of Zone CN10. In Holes 998A and 1000A, the uppermost specimens of *Amaurolithus* observed belong to *A. primus*, whereas in Hole 999A, they are *A. tricorniculatus* specimens.

Zone CN10 can be subdivided into three subzones at the sites investigated. The boundary between Subzones CN10c (*Ceratolithus rugosus* Subzone) and CN10b (*Ceratolithus acutus* Subzone) is defined by the FO of *C. rugosus* as well as the LO of *C. acutus* (Bukry,

1973). The FO of *C. rugosus* is more easily determined in the Caribbean sections, however, Raffi and Flores (1995) indicated that this event is slightly diachronous with respect to magnetostratigraphy.

C. acutus has a continuous distribution in the lower Pliocene section in the three holes and the FO of this species is used to define the boundary between Subzones CN10b and CN10a (*Triquetrorhabdulus rugosus* Subzone). This boundary is also defined by the LO of *T. rugosus* (Bukry, 1973), although this datum lies just below the FO of *C. acutus* in Holes 998A and 999A. Moreover, *T. rugosus* has a sporadic occurrence in Hole 1000A.

The Miocene/Pliocene boundary is placed within Subzone CN10a (e.g., Mazzei et al., 1979; Raffi and Flores, 1995).

Miocene

CN9 (*Discoaster quinqueramus* Zone)

Hole 998A: interval 165-998A-12H-1, 19 cm, to 14H-3, 20 cm
Hole 999A: interval 165-999A-18H-7, 30 cm, to 26H-2, 22 cm
Hole 1000A: interval 165-1000A-21H-2, 50 cm, to 31H-5, 50 cm

This interval lies between the FO of *Discoaster berggrenii* and the LO of *D. quinqueramus*. Both species are common in upper Miocene sediments in the Caribbean. Three datums, based on the FO and LOs of species of *Amaurolithus*, can be used to subdivide this zone. Bukry (1973, 1975; Okada and Bukry, 1980) divided Zone CN9 into Subzones CN9b (*Amaurolithus primus* Subzone) and CN9a (*Discoaster berggrenii* Subzone) by the FO of *Amaurolithus primus*. Raffi and Flores (1995) used the FO of *Amaurolithus* spp. to subdivide this interval into two subzones. *A. primus* is rare in the sections studied, but the FO of *Amaurolithus delicatus* can be determined precisely in Holes 998A and 1000A, and thus we use this event to determine the base of Subzone CN9b. In addition, the FO and LO of *Amaurolithus amplifucus* lie within Subzone CN9b and can be used to subdivide this subzone at the Caribbean sites into three biostratigraphic units (CN9bA, CN9bB, and CN9bC in ascending order) following Raffi and Flores (1995).

Specimens of *Reticulofenestra* >7 µm in diameter (*R. pseudoumbilicus*) are observed above the lower part of Subzone CN9b in Holes 998A and 1000A and above the middle part of Subzone CN9a in Hole 999A (Figs. 5, 6). The temporary disappearance of this taxon in the lower part of Zone CN9 and the upper part of Zone CN8, the small *Reticulofenestra* event or the paracme interval of *R. pseudoumbilicus*, has also been observed in the equatorial Indian Ocean (Rio et al., 1990; Young, 1990), in the western equatorial Pacific Ocean (Takayama, 1993), the eastern equatorial Pacific (Raffi and Flores, 1995), and the western equatorial Atlantic (Backman and Raffi, 1997). The reappearance of *R. pseudoumbilicus* (>7 µm in diameter) in Zone CN9 is used by Raffi and Flores (1995) to define the top of the paracme interval of *R. pseudoumbilicus*.

The LO of *Minylitha convallis* lies in Subzone CN9a in Holes 998A and 999A; this event is difficult to determine in Hole 1000A because of poor preservation.

CN8 (*Discoaster neohamatus* Zone)

Hole 998A: interval 165-998A-14H-3, 100 cm, to 15H-3, 100 cm
Hole 999A: interval 165-999A-26X-2, 100 cm, to 29X-1, 22 cm
Hole 1000A: interval 165-1000A-31H-6, 50 cm, to 36X-6, 50 cm

This interval lies between the LO of *Discoaster hamatus* and the FO of *D. berggrenii*. Zone CN8 is subdivided into Subzones CN8b (*Discoaster neorectus* Subzone) and CN8a (*Discoaster bellus* Subzone) by the FO of *Discoaster loeblichii*. This datum can be determined in Holes 998A and 999A although *D. loeblichii* is rare in both holes. It is hard to distinguish this species from other poorly preserved species of *Discoaster* in Hole 1000A.

In Holes 998A and 999A, the FO of *M. convallis* lies near the LO of *D. hamatus*. This event was recognized near the base of Zone CN8 in the eastern equatorial Pacific and the Indian Ocean (Raffi et al., 1995).

CN7 (*Discoaster hamatus* Zone)

Hole 998A: interval 165-998A-15H-4, 20 cm, to 16H-5, 100 cm
Hole 999A: interval 165-999A-29X-1, 100 cm, to 29X-CC
Hole 1000A: interval 165-1000A-36X-CC, to 40X-6, 50 cm

Zone CN7 (*Discoaster hamatus* Zone) corresponds to the total range of *Discoaster hamatus*. *D. hamatus* is abundant in the three holes and thus its range can be determined precisely.

Bukry (1973) used the FO of *Catinaster calyculus* to define the boundary between Subzones CN7b (*Catinaster calyculus* Subzone) and CN7a (*Helicosphaera carteri* Subzone). However, in Holes 999A and 1000A this event lies below the FO of *D. hamatus*. A similar relationship was observed in the eastern equatorial Pacific (Raffi and Flores, 1995), in the western Indian Ocean (Rio et al., 1990), and in the Ceara Rise (Backman and Raffi, 1997). The LO of *C. calyculus* lies in Zone CN7 in all three holes, but this event is not considered to be reliable because of its sporadic occurrence.

Zone CN6 (*Catinaster coalitus* Zone)

Hole 998A: interval 165-998A-16H-6, 20 cm, to 16H-CC
Hole 999A: interval 165-999A-30X-1, 22 cm, to 30X-5, 21 cm
Hole 1000A: interval 165-1000A-40X-CC, to 41X-5, 50 cm

The base of this zone corresponds to the FO of *Catinaster coalitus*. This species is common in Holes 998A, 999A, and 1000A, therefore, the lower limit of CN6 can be determined precisely. The LO of *Coccolithus miopelagicus* lies in Zone CN6 in all three holes; this datum lies just below the top of the zone in Holes 998A and 1000A.

Nannofossils are typically poorly preserved in this zone, which corresponds to the "carbonate crash" (Lyle et al., 1995).

CN5 (*Discoaster exilis* Zone)

Hole 998A: interval 165-998A-17H-1, 20 cm, to 19X-5, 20 cm
Hole 999A: interval 165-999A-30X-5, 100 cm, to 37X-5, 100 cm
Hole 1000A: interval 165-1000A-41X-6, 50 cm, to 55X-6, 50 cm

This interval lies between the LO of *Spinelithus heteromorphus* and the FO of *Catinaster coalitus*. Bukry (1973) also used the LO of *Discoaster kugleri* to define the top of Zone CN5. We do not use this event as the zonal boundary for the top of Zone CN5 because the LO of *D. kugleri* lies below the FO of *C. coalitus* in the three holes studied.

The FO of *Discoaster kugleri* has been used to subdivide Zone CN5 into Subzones CN5b (*D. kugleri* Subzone) and CN5a (*Coccolithus miopelagicus* Subzone) (Bukry, 1973, 1975). Because *D. kugleri* is rare in the lower part of its range, we cannot determine its FO precisely. We can determine the abundance increase of *D. kugleri*, an event that has been used by Raffi and Flores (1995).

Other stratigraphically useful bioevents in Zone CN5 in the Caribbean sites include the LOs of *Cyclicargolithus floridanus* and *Coronocyclus nitescens*. The LO of *C. floridanus* was defined by Bukry (1973) as an alternate marker for the base of Subzone CN5b. However, this event lies in Subzone CN5a, just above the base of Zone CN5. This event was also recognized in higher levels in the North Atlantic (Takayama and Sato, 1987; Gartner, 1992). The LO of *C. nitescens* was shown to be a useful event by Gartner and Chow (1985) and Fornaciari et al. (1990). This datum lies below the abundance increase

of *D. kugleri* in Holes 998A and 999A, but it cannot be determined in Hole 1000A because of poor preservation.

CN4 (*Sphenolithus heteromorphus* Zone)

Hole 998A: interval 165-998A-19X-5, 80 cm, to 21X-CC
 Hole 999A: interval 165-999A-37X-6, 22 cm, to 39X-7, 30 cm
 Hole 1000A: interval 165-1000A-55X-CC to below base of section

This interval lies between the LO of *Helicosphaera ampliaptera* and the LO of *Sphenolithus heteromorphus*. Both datums can be determined precisely in the three holes. The LO of *Discoaster deflandrei* lies in this zone. The abundance of *Discoaster signus* and *D. variabilis* increases abruptly in the upper part of CN4.

CN3 (*Helicosphaera ampliaptera* Zone)

Hole 998A: interval 165-998A-22X-1, 67 cm, to 26X-CC
 Hole 999A: interval 165-999A-39X-CC, to 48X-CC

This interval lies between the FO of *Sphenolithus heteromorphus* and the LO of *Helicosphaera ampliaptera* and can be recognized in Holes 998A and 999A. Bukry (1973, 1975, 1978) suggested the use of the FO of *Calcidiscus macintyreii* to define the boundary between Zones CN4 and CN3. However, this species is completely absent from both zones in the Caribbean sections. Another datum used to define the upper boundary of CN3 by Bukry (1973, 1975) is the top of the acme of *D. deflandrei*. However, this event is highly dependent on preservation and lies below the LO of *H. ampliaptera* in the three holes studied, the same as observed in the Atlantic (e.g., Olafsson, 1991; Gartner, 1992) and the eastern equatorial Pacific (Raffi and Flores, 1995).

CN2 (*Sphenolithus belemnus* Zone)

Hole 998A: interval 165-998A-27X-1, 100 cm, to 28X-3, 100 cm
 Hole 999A: interval 165-999A-49X-1, 100 cm, to 51X-CC

This interval lies between the FO of *Sphenolithus belemnus* and the FO of *S. heteromorphus*. *Discoaster deflandrei*, *Coccolithus miope-lagicus*, *Cyclicargolithus floridanus*, and *Sphenolithus moriformis* are common in this zone.

CN1 (*Triquetrorhabdulus carinatus* Zone)

Hole 998A: interval 165-998A-28X-4, 100 cm, to 36X-2, 100 cm
 Hole 999A: interval 165-999A-52X-1, 100 cm, to below base of section

This interval lies between the LO of *Reticulofenestra bisecta* and the FO of *Sphenolithus belemnus*. Because *Discoaster druggii* and *Cyclicargolithus abisectus* have sporadic distributions in the Caribbean sections, we cannot subdivide this zone into subzones as proposed by Bukry (1973, 1975). The LOs of *Triquetrorhabdulus carinatus* and *Sphenolithus delphix* can be determined precisely in Hole 998A.

The LO of *Sphenolithus delphix* lies close to the Oligocene/Miocene boundary (Fornaciari and Rio, 1996).

STRATIGRAPHIC SIGNIFICANCE OF RETICULOFENESTRA COCCOLITHS

Size Variation of *Reticulofenestra* Coccoliths during the Neogene

Distinctive changes in the size of specimens of the Neogene genus *Reticulofenestra* have been observed by numerous authors. Young

(1990) studied size distribution patterns in the middle Miocene to Pliocene *Reticulofenestra* specimens in the western Indian Ocean and the Red Sea, and was the first to define the small *Reticulofenestra* event (SRE), in which the specimens $>5\mu\text{m}$ in size virtually disappear in late Miocene Zones NN9 (CN8) and NN11 (CN9). Rio et al. (1990) identified the "paracme of *Reticulofenestra*" based on the disappearance of large ($>7\mu\text{m}$ in diameter) specimens of *Reticulofenestra* from Zone CN8 to the middle of Zone CN9 in Indian Ocean sediments. Takayama (1993) divided various *Reticulofenestra* species into four groups based on their sizes and showed characteristic stratigraphic distribution patterns of them throughout the Neogene.

We measured the size and shape of *Reticulofenestra* coccoliths in Zones CN3 to CN12 from Holes 998A and 999A. Based on these data, we observed intervals where there are distinctive changes. We can define several new biostratigraphic events based on these changes as well as observe the size changes proposed by Takayama (1993). We recognized three major intervals within the Neogene sections studied, from top to bottom: Intervals I, II, and III.

Interval I: Zone CN12

This interval corresponds to Zone CN12 in Holes 998A and 999A. In this interval, medium (5–7 μm in diameter), small (3–5 μm in diameter) and very small ($<3\mu\text{m}$ in diameter) *Reticulofenestra* specimens are observed. Interval I corresponds to the upper part of Interval A1 of Takayama (1993). Four biostratigraphic units were recognized in this interval based on abrupt decreases in size and/or sudden disappearance of characteristic species of *Reticulofenestra*.

Interval Ia: Subzone CN12d

This interval is characterized by the dominant occurrence of very small specimens of *Reticulofenestra* ($<3\mu\text{m}$ in diameter) with few larger specimens ($>6\mu\text{m}$ in diameter; Figs. 5, 6).

Interval Ib: Subzones CN12c to CN12b

The upper boundary of this interval is defined by the abrupt and temporal disappearance of larger specimens of *Reticulofenestra* (6–7 μm in diameter in Hole 998A and 5–7 μm in diameter in Hole 999A). These specimens are present characteristically in the upper part of this interval, whereas the lower part of the interval is characterized by small to medium *Reticulofenestra* specimens (Figs. 5, 6).

Interval Ic: Upper Part of Subzone CN12a

The upper boundary of this interval is defined by the disappearance of *Reticulofenestra ampla*. This horizon lies close to the LO of *Discoaster tamalis* (Sato et al., 1991; Kameo et al., 1995), the boundary between Subzones CN12c and CN12b. *R. ampla*, described by Sato et al. (1991) in the Indian and the North Atlantic Oceans, is an elliptical medium-sized species ($>5\mu\text{m}$ in diameter) and is similar to but smaller than *R. pseudoumbilicus*. The former species characteristically is in the uppermost part of Subzone CN12a and disappears near the LO of *D. tamalis*. Throughout this interval, small to very small specimens of *Reticulofenestra* are abundant (Figs. 5, 6).

Interval Id: Lower Part of Subzone CN12a

In the lower part of Subzone CN12a, relatively large specimens (6–7 μm in diameter) of *Reticulofenestra* are observed. These larger specimens include circular forms of *Reticulofenestra* that suddenly disappear within Subzone CN12a in Holes 998A, 999A, and 1000A. This circular form is assigned to a variety of *Reticulofenestra minutula*. Small to very small specimens are also abundant in this interval (Figs. 5, 6).

Interval II: Zones CN11 to CN8

This interval lies in Zone CN11 to the middle part of Zone CN8 (middle Miocene to lower Pliocene). We have defined three subintervals (Figs. 5, 6).

Interval IIa: CN11 to the Lower Part of Subzone CN10b

The upper boundary of this interval corresponds to the LO of *R. pseudoubilicus*. In the lower part of the interval, medium-sized *Reticulofenestra* specimens (5–7 μm in diameter) are dominant, whereas the middle to upper part of this interval contains smaller sized *Reticulofenestra* specimens with some larger sized specimens. Interval IIa closely correlates to the lower part of Interval A1 of Takayama (1993; Figs. 5, 6).

Interval IIb: Lowest Part of Subzone CN10b to Middle Part of Zone CN9

The upper boundary of this interval is characterized by the temporary disappearance of larger specimens of *Reticulofenestra* (>10 μm in diameter in Hole 998A and 7 μm in diameter in Hole 999A) near the base of Subzone CN10b (Figs. 5, 6). In this interval, small to large *Reticulofenestra* specimens (>3 μm in diameter) are dominant, whereas very small *Reticulofenestra* specimens (<3 μm in diameter) are rare. This interval corresponds to the upper part of Interval A2 of Takayama (1993).

Interval IIc: Middle Part of Zone CN9 to Lower Part of Subzone CN8b

The boundary between Intervals IIb and IIc is defined by the reentrance of common large (>7 μm in diameter) specimens of *Reticulofenestra*. This interval is dominated by small to very small specimens of *Reticulofenestra* (<5 μm in diameter), whereas Interval IIb contains abundant medium to large specimens (Figs. 5, 6). The upper boundary of this interval lies in Subzone CN9b in Hole 998A and Subzone CN9a in Hole 999A. This difference may be caused by uncertainties in the FO of *Amaurolithus* spp. in Hole 999A, the event that defines the boundary between Subzones CN9b and CN9a. The lowermost common occurrence of larger *Reticulofenestra* specimens correlates to the top of the paracme of *R. pseudoubilicus* as defined by Rio et al. (1990) and Raffi and Flores (1995).

Interval III: Lower Part of Zone CN8 to Middle Part of Zone CN3

This interval corresponds to Zones CN8 through CN3. Large specimens of *Reticulofenestra* are common. There are two subintervals (Figs. 5, 6).

Interval IIIa: Lowermost Part of Subzone CN8b to Zone CN6

This interval is characterized by the dominance of medium to large specimens of *Reticulofenestra* (>5 μm in diameter), whereas small to very small *Reticulofenestra* specimens (<5 μm in diameter) are very rare to absent (Figs. 5, 6). The upper boundary of this interval corresponds to the abrupt disappearance of large specimens of *Reticulofenestra* near the base of Subzone CN8b. This dramatic event is called the base of paracme of *R. pseudoubilicus* by Rio et al. (1990) and Raffi and Flores (1995) and can be identified in the three holes studied.

Interval IIIb: Zones CN5 to CN3

This interval contains small to medium specimens of *Reticulofenestra* (3–7 μm in diameter). Very small specimens of *Reticulofenestra* (<3 μm in diameter) are rare (Figs. 5, 6). The upper boundary of this interval is characterized by the abrupt decrease in the abundance of small specimens of *Reticulofenestra* near the base of Zone CN6. In the lower part of this interval, large *Reticulofenestra* specimens are rare.

Remarks on Stratigraphic Meaning of *Reticulofenestra* Events

We have recognized the size variations in specimens of *Reticulofenestra* in the stratigraphic interval from CN3 to CN12 that can be correlated between the Caribbean sites (Figs. 5, 6). The patterns of

size variations include cyclic changes in the relative abundance of the different size groups as well as changes in the maximum size of the specimens. For example, in Interval III (Zones CN3–CN4), small to medium (<5 μm in diameter) specimens of *Reticulofenestra* are common. The maximum size of specimens increases upward, exceeding 10 μm in Zone CN5. At the same time, medium to large specimens become the most common size group. This upward increase in maximum size of specimens is a characteristic trend in the evolution of Neogene *Reticulofenestra*. Interval II seems to include two cycles in the increase in maximum size. The lower cycle corresponds to Intervals IIc to IIb and the upper cycle is the middle part of Intervals IIb to IIa. Interval I is more complicated and contains several short cycles of variations in size superimposed on an upward increase in the maximum size of specimens.

We propose eight datums based on *Reticulofenestra* size variation that are stratigraphically useful (listed in descending order):

1. Abrupt and temporal disappearance of medium-sized specimens (the boundary of Intervals Ia and Ib): This event is placed near the boundary of Subzones CN12d and CN12c.
2. LO of *R. ampla* (the boundary of Intervals Ib and Ic): This event is the disappearance of elliptical and medium *Reticulofenestra* specimens and is placed near the LO of *D. tamalis*.
3. LO of a circular form of *Reticulofenestra minutula* (the boundary of Intervals Ic and Id): This event is the abrupt disappearance of circular, medium-sized specimens and is situated in the middle of Subzone CN12a.
4. LO of *R. pseudoubilicus* (the boundary of Intervals I and II): This event corresponds to the boundary of Zones CN12 and CN11.
5. Abrupt decrease in the maximum size of *Reticulofenestra* (the boundary of Intervals IIa and IIb): This event is the disappearance of largest specimens (>10 μm) and is placed near the base of Subzone CN10b.
6. Reappearance of large *Reticulofenestra* specimens in the upper Miocene (the boundary of Intervals IIb and IIc): This event is the top of paracme of *R. pseudoubilicus*. It is placed within Zone CN9.
7. Sudden and temporary disappearance of large *Reticulofenestra* (the boundary of Intervals II and III): This event is the base of paracme of *R. pseudoubilicus* and is situated near the base of Subzone CN8b.
8. Decrease in the abundance of small specimens of *Reticulofenestra* (the boundary of Intervals IIIa and IIIb): This event is placed near the base of Zone CN6.

CONCLUSIONS

A total of 53 calcareous nannofossil datums were determined in Neogene and Quaternary sections in Holes 998A, 999A, and 1000A in the Caribbean Sea.

Stratigraphic changes in the size distribution of *Reticulofenestra* were determined. Some of the abrupt changes recognized have the potential to be reliable events during the Neogene.

ACKNOWLEDGMENTS

We are grateful to Drs. Haraldur Sigurdsson, R. Mark Leckie, Gary D. Acton, William P. Chaisson, Steven L. D'Hondt, and other shipboard scientists on Leg 165 who provided encouragement, friendship, and valuable advice. We are also grateful to Drs. Katharina von Salis Perch-Nielsen and Isabella Raffi for constructive reviews of this paper.

REFERENCES

- Backman, J., and Raffi, I., 1997. Calibration of Miocene nannofossil events to orbitally tuned cyclostratigraphies from Ceara Rise. In Shackleton, N.J., Curry, W.B., Richter, C., and Bralower, T.J. (Eds.), *Proc. ODP, Sci. Results*, 154: College Station, TX (Ocean Drilling Program), 83–99.
- Backman, J., Schneider, D.A., Rio, D., and Okada, H., 1990. Neogene low-latitude magnetostratigraphy from Site 710 and revised age estimates of Miocene nannofossil datum events. In Duncan, R.A., Backman, J., Peterson, L.C., et al., *Proc. ODP, Sci. Results*, 115: College Station, TX (Ocean Drilling Program), 271–276.
- Backman, J., and Shackleton, N.J., 1983. Quantitative biochronology of Pliocene and early Pleistocene calcareous nannofossils from the Atlantic, Indian and Pacific oceans. *Mar. Micropaleontol.*, 8:141–170.
- Berggren, W.A., Kent, D.V., Swisher, C.C., III, and Aubry, M.-P., 1995. A revised Cenozoic geochronology and chronostratigraphy. In Berggren, W.A., Kent, D.V., Aubry, M.-P., and Hardenbol, J. (Eds.), *Geochronology, Time Scales and Global Stratigraphic Correlation*. Spec. Publ.—Soc. Econ. Paleontol. Mineral. (Soc. Sediment. Geol.), 54:129–212.
- Bukry, D., 1973. Low-latitude coccolith biostratigraphic zonation. In Edgar, N.T., Saunders, J.B., et al., *Init. Repts. DSDP*, 15: Washington (U.S. Govt. Printing Office), 685–703.
- , 1975. Coccolith and silicoflagellate stratigraphy, northwestern Pacific Ocean, Deep Sea Drilling Project Leg 32. In Larson, R.L., Moberly, R., et al., *Init. Repts. DSDP*, 32: Washington (U.S. Govt. Printing Office), 677–701.
- , 1978. Biostratigraphy of Cenozoic marine sediment by calcareous nannofossils. *Micropaleontology*, 24:44–60.
- , 1991. Paleoeological transect of western Pacific Ocean late Pliocene coccolith flora. Part I: Tropical Ontong-Java Plateau at ODP 806B. *Open-File Rep.-U.S. Geol. Surv.*, 91-552: 1–35.
- Cande, S.C., and Kent, D.V., 1995. Revised calibration of the geomagnetic polarity timescale for the Late Cretaceous and Cenozoic. *J. Geophys. Res.*, 100:6093–6095.
- Curry, W.B., Shackleton, N.J., Richter, C., et al., 1995. *Proc. ODP, Init. Repts.*, 154: College Station, TX (Ocean Drilling Program).
- Flores, J.-A., Sierro, F.J., and Raffi, I., 1995. Evolution of the calcareous nannofossil assemblage as a response to the paleoceanographic changes in the eastern equatorial Pacific Ocean from 4 to 2 Ma (Leg 138, Sites 849 and 852). In Pisias, N.G., Mayer, L.A., Janecek, T.R., Palmer-Julson, A., and van Andel, T.H. (Eds.), *Proc. ODP, Sci. Results*, 138: College Station, TX (Ocean Drilling Program), 163–176.
- Fornaciari, E., Raffi, I., Rio, D., Villa, G., Backman, J., and Olafsson, G., 1990. Quantitative distribution patterns of Oligocene and Miocene calcareous nannofossils from the western equatorial Indian Ocean. In Duncan, R.A., Backman, J., Peterson, L.C., et al., *Proc. ODP, Sci. Results*, 115: College Station, TX (Ocean Drilling Program), 237–254.
- Fornaciari, E., and Rio, D., 1996. Latest Oligocene to early middle Miocene quantitative calcareous nannofossil biostratigraphy in the Mediterranean region. *Micropaleontology*, 42:1–36.
- Gartner, S., and Chow, J., 1985. Calcareous nannofossil biostratigraphy, Deep Sea Drilling Project Leg 85, eastern equatorial Pacific. In Mayer, L., Theyer, F., Thomas, E., et al., *Init. Repts. DSDP*, 85: Washington (U.S. Govt. Printing Office), 609–619.
- Gartner, S., 1992. Miocene nannofossil chronology in the North Atlantic, DSDP Site 608. *Mar. Micropaleontol.*, 18:307–331.
- Hay, W.W., and Towe, K.M., 1962. Electron microscope examination of some coccoliths from Donzaq (France). *Eclogae. Geol. Helv.*, 55:497–517.
- Kameo, K., Sato, T., and Takayama, T., 1995. Late Pliocene calcareous nannofossil datums and bioevents. In Flores, J.A., and Sierro, F.J. (Eds.), *Proc. 5th INA Conf.*, Universidad de Salamanca, 87–98.
- Lyle, M., Dadey, K.A., and Farrell, J.W., 1995. The late Miocene (11–8 Ma) eastern Pacific carbonate crash: evidence for reorganization of deep-water circulation by the closure of the Panama Gateway. In Pisias, N.G., Mayer, L.A., Janecek, T.R., Palmer-Julson, A., and van Andel, T.H. (Eds.), *Proc. ODP, Sci. Results*, 138: College Station, TX (Ocean Drilling Program), 821–838.
- Martini, E., 1971. Standard Tertiary and Quaternary calcareous nannoplankton zonation. In Farinacci, A. (Ed.), *Proc. 2nd Int. Conf. Planktonic Microfossils Roma*: Rome (Ed. Tecnosci.), 2:739–785.
- Mazzei, R., Raffi, I., Rio, D., Hamilton, N., and Cita, M.B., 1979. Calibration of late Neogene calcareous plankton datum planes with the paleomagnetic record of Site 397 and correlation with Moroccan and Mediterranean sections. In von Rad, U., Ryan, W.B.F., et al., *Init. Repts. DSDP*, 47 (Pt. 1): Washington (U.S. Govt. Printing Office), 375–389.
- Okada, H., and Bukry, D., 1980. Supplementary modification and introduction of code numbers to the low-latitude coccolith biostratigraphic zonation (Bukry, 1973; 1975). *Mar. Micropaleontol.*, 5:321–325.
- Olafsson, G., 1991. Quantitative calcareous nannofossil biostratigraphy and biochronology of early through late Miocene sediments from DSDP Hole 608. *Medd. Stockholm Univ. Inst. Geol. Geochem.*, 203.
- Raffi, I., Backman, J., Rio, D., and Shackleton, N.J., 1993. Plio-Pleistocene nannofossil biostratigraphy and calibration to oxygen isotope stratigraphies from Deep Sea Drilling Project Site 607 and Ocean Drilling Program Site 677. *Paleoceanography*, 8: 387–408.
- Raffi, I., and Flores, J.-A., 1995. Pleistocene through Miocene calcareous nannofossils from eastern equatorial Pacific Ocean. In Pisias, N.G., Mayer, L.A., Janecek, T.R., Palmer-Julson, A., and van Andel, T.H. (Eds.), *Proc. ODP, Sci. Results*, 138: College Station, TX (Ocean Drilling Program), 233–286.
- Raffi, I., Rio, D., d'Atri, A., Fornaciari, E., and Rocchetti, S., 1995. Quantitative distribution patterns and biomagnetostratigraphy of middle and late Miocene calcareous nannofossils from equatorial Indian and Pacific oceans (Leg 115, 130, and 138). In Pisias, N.G., Mayer, L.A., Janecek, T.R., Palmer-Julson, A., and van Andel, T.H. (Eds.), *Proc. ODP, Sci. Results*, 138: College Station, TX (Ocean Drilling Program), 479–502.
- Rio, D., 1982. The fossil distribution of coccolithophore genus *Gephyrocapsa* Kamptner and related Plio-Pleistocene chronostratigraphic problems. In Prell, W.L., Gardner, J.V., et al., *Init. Repts. DSDP*, 68: Washington (U.S. Govt. Printing Office), 325–343.
- Rio, D., Fornaciari, E., and Raffi, I., 1990. Late Oligocene through early Pleistocene calcareous nannofossils from western equatorial Indian Ocean (Leg 115). In Duncan, R.A., Backman, J., Peterson, L.C., et al., *Proc. ODP, Sci. Results*, 115: College Station, TX (Ocean Drilling Program), 175–235.
- Sato, T., Kameo, K., and Takayama, T., 1991. Coccolith biostratigraphy of the Arabian Sea. In Prell, W.L., Niitsuma, N., et al., *Proc. ODP, Sci. Results*, 117: College Station, TX (Ocean Drilling Program), 37–54.
- Sigurdsson, H., Leckie, R.M., Acton, G.D., et al., 1997. *Proc. ODP, Init. Repts.*, 165: College Station, TX (Ocean Drilling Program).
- Takayama, T., 1970. The Pliocene-Pleistocene boundary in the Lamont Core V-21-98 and at Le Castella, Southern Italy. *J. Mar. Geol.*, 6:70–77.
- , 1993. Notes on Neogene calcareous nannofossil biostratigraphy of the Ontong Java Plateau and size variations of *Reticulofenestra* coccoliths. In Berger, W.H., Kroenke, L.W., Mayer, L.A., et al., *Proc. ODP, Sci. Results*, 130: College Station, TX (Ocean Drilling Program), 179–229.
- Takayama, T., and Sato, T., 1987. Coccolith biostratigraphy of the North Atlantic Ocean, Deep Sea Drilling Project Leg 94. In Ruddiman, W.F., Kidd, R.B., Thomas, E., et al., *Init. Repts. DSDP*, 94 (Pt. 2): Washington (U.S. Govt. Printing Office), 651–702.
- Takayama, T., Sato, T., Kameo, K., and Goto, T., 1995. Quaternary coccolith biostratigraphy and the age of the Pliocene/Pleistocene boundary. *Quat. Res.*, 34: 157–170.
- Thierstein, H.R., Geitzenauer, K., Molino, B., and Shackleton, N.J., 1977. Global synchronicity of late Quaternary coccolith datum levels: validation by oxygen isotopes. *Geology*, 5:400–404.
- Young, J.R., 1990. Size variation of Neogene *Reticulofenestra* coccoliths from Indian Ocean DSDP cores. *J. Micropaleontol.*, 9:71–85.

Date of initial receipt: 17 June 1998

Date of acceptance: 11 January 1999

Ms 165SR-012

APPENDIX A

Twenty-three genera and 112 species recognized in this investigation of the core samples are listed below.

Amaurolithus amplificus (Bukry and Percival, 1971) Gartner and Bukry, 1975
Amaurolithus delicatus Gartner and Bukry, 1975
Amaurolithus primus (Bukry and Percival, 1971) Gartner and Bukry, 1975
Amaurolithus tricorniculatus (Gartner, 1967) Gartner and Bukry, 1975
Calcidiscus leptoporus (Murray and Blackman, 1898) Loeblich and Tappan, 1978
Calcidiscus macintyreii (Bury and Bramlette, 1969) Loeblich and Tappan, 1978
Calcidiscus premacintyreii Theodoridis, 1984
Catinaster calyculus Martini and Bramlette, 1963
Catinaster coalitus Martini and Bramlette, 1965
Catinaster mexicanus Bukry, 1971
Ceratolithus acutus Gartner and Bukry, 1974
Ceratolithus cristatus Kamptner, 1950
Ceratolithus rugosus Bukry and Bramlette, 1968
Ceratolithus simplex Bukry, 1979
Ceratolithus telesmus Norris, 1965
Coccolithus crassipons Bouché, 1962
Coccolithus miopelagicus Bukry, 1971
Coccolithus pelagicus (Wallich, 1877) Schiller, 1930
Coccolithus streckerii Takayama and Sato, 1987
Coronocyclus nitescens (Kamptner, 1963) Bramlette and Wilcoxon, 1967
Cyclicargolithus floridanus (Roth and Hay in Hay et al., 1967) Bukry, 1971
Cyclolithella annula (Cohen, 1964) McIntyre and Bé, 1967
Dictyococcites spp.
Remarks. In the present study, all reticulofenestrid specimens whose central opening cannot be identified under the light microscope are included into “*Dictyococcites*” specimens.
Discoaster adamanteus Bramlette and Wilcoxon, 1967
Discoaster asymmetricus Gartner, 1969
Discoaster bellus Bukry and Percival, 1971
Discoaster berggrenii Bukry, 1971
Discoaster bollii Martini and Bramlette, 1963
Discoaster brouweri Tan (1927) emend. Bramlette and Riedel, 1954
Discoaster calcaris Gartner, 1967
Discoaster calculosus Bukry, 1971
Discoaster challengerii Bramlette and Riedel, 1954
Discoaster decorus (Bukry, 1971) Bukry, 1973
Discoaster deflandrei Bramlette and Riedel, 1954
Discoaster drugii Bramlette and Wilcoxon, 1967
Discoaster exilis Martini and Bramlette, 1963
Discoaster hamatus Martini and Bramlette, 1963
Discoaster icarus Stradner, 1973
Discoaster intercalaris Bukry, 1971
Discoaster kugleri Martini and Bramlette, 1963
Discoaster loeblichii Bukry, 1971
Discoaster moorei Bukry, 1971
Discoaster musicus Stradner, 1959
Discoaster neohamatus Bukry and Bramlette, 1963
Discoaster neorectus Bukry, 1971
Discoaster pansus (Bukry and Percival, 1971) Bukry, 1973
Discoaster pentaradiatus Tan (1927) emend. Bramlette and Riedel, 1954
Discoaster perclarus Haq in Haq et al., 1967
Discoaster prepentaradiatus Bukry and Percival, 1971
Discoaster pseudovariabilis Martini and Worsley, 1971
Discoaster quadramus Bukry, 1973
Discoaster quinqueramus Gartner, 1969
Discoaster signus Bukry, 1971
Discoaster surculus Martini and Bramlette, 1963
Discoaster tamalis Kamptner, 1967
Discoaster triradiatus Tan, 1927
Discoaster variabilis Martini and Bramlette, 1963
Discolithina japonica Takayama, 1967
Discolithina multipora (Kamptner, 1948) Roth, 1970
Emilianina huxleyi (Lohmann, 1902) Hay and Mohler in Hay et al., 1967
Gephyrocapsa caribbeanica Boudreaux and Hay, 1967

Remarks: This species was identified by characteristic features of its size (4–6 µm in length) and orientation of the diagonal bar (>45° with short axis).

Gephyrocapsa oceanica Kamptner, 1943

Remarks: This species was identified by characteristic features of its size (4–6 µm in length) and orientation of the diagonal bar (<45° with short axis).

Gephyrocapsa parallela Hay and Beaudry, 1973

Gephyrocapsa spp. (large).

Remarks: Specimens of *G. oceanica* and *G. caribbeanica* >6 µm in length are included into *Gephyrocapsa* spp. (large).

Gephyrocapsa spp. (small)

Remarks: Calcareous nannofossil assemblages in the upper Pliocene and other intervals in the studied sections are characterized by the dominance of *Gephyrocapsa* specimens. All of these *Gephyrocapsa* are <4 µm in length. In the present study, they are included in “small” *Gephyrocapsa*.

Helicosphaera ampliapertura Bramlette and Wilcoxon, 1967

Helicosphaera carteri (Wallich, 1877) Kamptner, 1954

Helicosphaera euphratis Haq, 1966

Helicosphaera granulata Bukry and Percival, 1971

Helicosphaera hyalina Gaarder, 1970

Helicosphaera inversa Gartner, 1980

Helicosphaera neogranulata Gartner, 1977

Helicosphaera obliqua Bramlette and Wilcoxon, 1967

Helicosphaera orientalis Black, 1971

Helicosphaera scissura Miller, 1981

Helicosphaera sellii Bukry and Bramlette, 1969

Helicosphaera stalis Theodoridis, 1984

Helicosphaera wallichii (Lohmann, 1902) Boudreaux and Hay, 1969

Minylitha convallis Bukry, 1973

Oolithotus antillarum (Cohen, 1964) Reinhardt, 1968

Pseudoemiliania lacunosa (Kamptner, 1963) Gartner, 1969

Pyrocyclus sp.

Remarks: Genus *Pyrocyclus* was defined by Hay and Towe (1962) as a small coccolith of a single shield with a central opening. In the present study, specimens that consist of a single shield with a central opening are treated as *Pyrocyclus* sp.

Reticulofenestra ampla Sato, Kameo and Takayama, 1991

Reticulofenestra asanoi Sato and Takayama, 1992

Reticulofenestra bisectus (Hay, Mohler and Wade, 1966) Bukry and Percival (1971)

Reticulofenestra minuta Roth, 1970

Reticulofenestra minutula (Gartner, 1967) Haq and Berggren, 1978

Reticulofenestra minutula (circular form)

Remarks: In the present study, circular forms of *Reticulofenestra minutula* were characteristically observed in mid-Pliocene sequences, and they are usually >5 µm in length. Thus, the specimens are called *R. minutula* (circular form).

Reticulofenestra pseudoumbilicus (Gartner, 1967) Gartner, 1969

Rhabdosphaera clavigera Murray and Blackman, 1898

Rhabdosphaera longistylis Schiller, 1925

Rhabdosphaera stylifera (Lohmann, 1902) Boudreaux and Hay, 1969

Scapholithus fossilis Deflandre in Deflandre and Fert, 1954

Sphenolithus abies Deflandre in Deflandre and Fert, 1954

Sphenolithus belemnus Bramlette and Wilcoxon, 1967

Sphenolithus capricornutus Bukry and Percival, 1971

Sphenolithus conicus Bukry 1971

Sphenolithus delphix Bukry, 1973

Sphenolithus dissimilis Bukry and Percival, 1971

Sphenolithus heteromorphus Deflandre, 1953

Sphenolithus moriformis (Brönnimann and Stradner, 1960) Bramlette and Wilcoxon, 1967

Sphenolithus neoabies Bukry and Bramlette, 1969

Syracosphaera pulchra Lohmann, 1902

Syracosphaera spp.

Tetralithoides symeonidesii Theodoridis, 1984

Triquetrorhabdulus carinatus Martini, 1965

Triquetrorhabdulus extensus Theodoridis, 1984

Triquetrorhabdulus rugosus Bramlette and Wilcoxon, 1967

Umbilicosphaera sibogae (Weber-can Bosse, 1901) Gaarder, 1970